Pergamon

PII: S0191-8141(96)00083-1

Journal of Structural Geology, Vol. 19, No. 1, pp. 89 to 98, 1997

0191-8141/97 $17.00 + 0.00

The effect of cover composition on extensional faulting above re-activated basement faults: results from analogue modelling

R. I. HIGGINS and L. B. HARRIS

Structural Geology Analogue Modelling Laboratory, Department of Geology and Geophysics, The University of Western Australia, Nedlands, WA 6907, Australia

(*Received* 21 *March* 1995; *accepted in revised form* 10 *September* 1996)

Abstract—Analogue models were used to investigate differences in deformation between sedimentary cover sequences of contrasting composition above reactivated basement faults during extension. Two types of model arrangements were used. The first represented clastic sediments directly overlying faulted basement, and the second represented a basal ductile layer in an overburden overlying the same faulted basement. The basement configuration consisted of faults both oblique and orthogonal to the bulk extension direction. Particular attention was paid to the resulting map-view fault patterns.

In experiments without a basal ductile layer in the overburden, grabens only developed in areas directly above basement faults. In section, cover faults above oblique basement faults curved in profile and, in places, exhibited reverse movement at shallow depth. In experiments involving a ductile layer at the base of the overburden, faults developed oblique to both the bulk extension direction and the basement faults. The resulting fault pattern was influenced by both bulk extension and basement fault reactivation.

The results indicate that cover sequences that include thick basal ductile layers above reactivated basement faults are more likely to develop faults with strikes perpendicular to the regional extension direction, compared to those without. Faulting in an overburden lacking a basal ductile sequence is more likely to be directly influenced by the underlying reactivated basement faults.

INTRODUCTION

Pre-existing faults are often zones of weakness, with reduced cohesive strength, internal friction and sliding friction compared to the surrounding intact rock. These zones fail preferentially during favourable subsequent deformation, often under stress levels lower than those needed for the creation of new faults (Krantz, 1989). Structures that develop in a sediment pile overlying basement faults during reactivation are often influenced by those basement faults, and more information on the effects of both cover sequence composition and basement fault geometry on syn-tectonic structures is needed.

Analogue modelling provides a powerful graphic and kinematic tool for studying progressive deformation which cannot be observed in nature. The basis of experimental modelling of the Earth's geological structures is the consistency of mechanical behaviour throughout a wide range of rock types and the similarity of deformation patterns in all scales of observation. Workers such as Tchalenko (1970) and Davy *et al.* (1990) have illustrated how fault patterns can show a degree of self similarity over a wide range of scales, a phenomenon underlying the worth of scaled analogue models. With the use of analogue models this paper investigates the plan-view geometry of structures produced in different types of cover above reactivated basement faults orthogonal and oblique to the applied extension. The difference in cover composition investigated here is the presence or absence of a basal ductile layer such as might be represented in nature as an evaporite or shale. Many authors have illustrated decoupling of a cover sequence from underlying basement by basal ductile layers using analogue models (Richard and Krantz, 1991; Vendeville *et al.*, 1994), but most analyse the experiments using section-views and a plan-view approach is lacking.

EXPERIMENTAL BACKGROUND

Apparatus and method

Experiments were performed using a deformation apparatus consisting of a screw-jack, a movable end-wall, a stationary end and a rubber sheet above a wood platform (Fig. 1a). At one end of the apparatus the rubber is connected to a sturdy block of wood (referred to as the moveable end-wall), which in turn is connected to a screw-jack. The screw-jack is operated by a computer-controlled stepping motor which allows precise control of the extension rate. At the other end of the rig (referred to as the stationary end), the rubber is clamped to the platform over which it slides. Models sat upon the rubber sheet and comprised a silicone putty layer of relatively high viscosity underlying a clay slab, into which cuts were made to represent faults in crystalline basement (Fig. 1b). Some experiments incorporated a thin layer of viscous silicone putty (but of lower viscosity than the basal putty) directly upon the clay to represent a ductile basal layer within a sedimentary sequence such as an evaporite or shale (Fig. 1c). The uppermost part of the model consisted of coloured layers of dry quartz sand, representing a clastic sedimentary sequence. Many workers have previously used silicone putty and sand to model

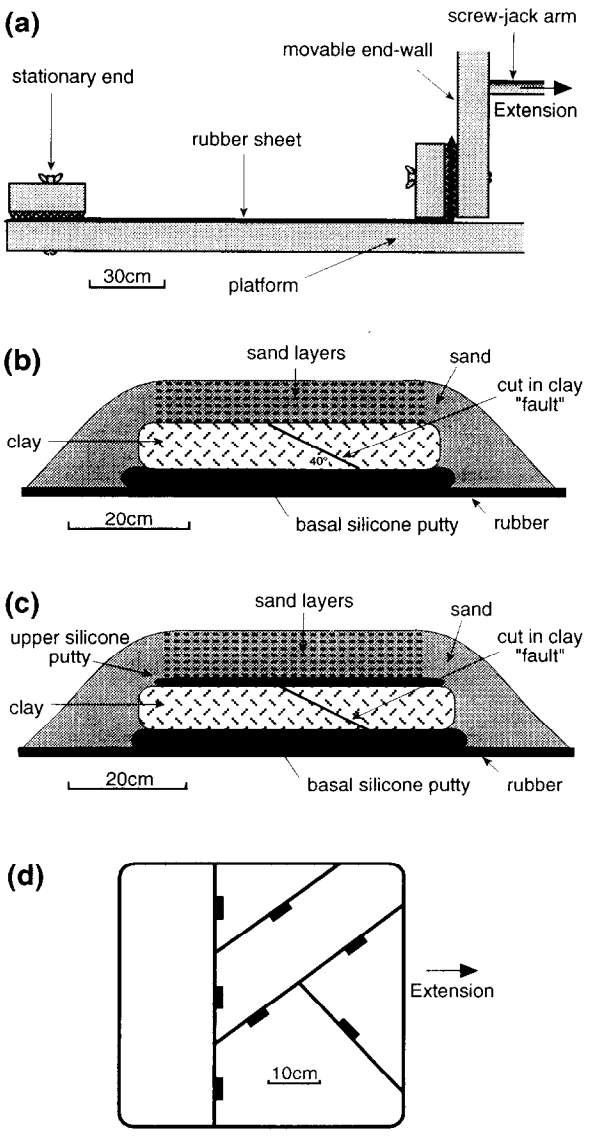

Fig. 1. (a) Experimental apparatus. (b) Schematic side-view diagram of the vertical arrangement of materials used to simulate the natural system, without a ductile layer in the cover, and (c) including the ductile layer. (d) Plan-view of geometry of pre-cut faults in the clay basement. All faults dip at 40°.

ductile and brittle sedimentary rocks, respectively (Vendeville *et al.*, 1986; Richard, 1991; Tron and Brun, 1991; Richard and Krantz, 1995; Vendeville *et al.*, 1995).

Before the model was prepared, talcum powder was spread under the rubber sheet to reduce friction at the base of the apparatus and thus allow uniform stretching of the sheet. After the basal silicone putty was rolled to size (20 mm thick) and positioned on the rubber, the desired fault geometry was cut into a 50 cm × 45 cm clay slab. Cuts were made so that faults were both orthogonal and oblique to the direction of bulk extension in the pattern shown in Fig. 1(d). The clay blocks were then allowed to dry to prevent them from sticking together. Because the clay blocks were dry and rigid, no internal deformation was possible. Lines were marked across the basement faults so that displacement across them could be measured after extension, and fault surfaces were smeared with vaseline to promote slippage. For experimental ease, all faults were cut straight with dips of 40°. If faults are cut at angles of greater than 40–50°, fault reactivation is not simulated as the clay blocks simply separate across the cut during extension. With faults cut at angles of less than 40–50°, there is sufficient weight of the overhanging portion of the hangingwall to keep it in contact with the footwall, allowing downward movement during extension. Thus no gap forms between the footwall and hangingwall. This effectively simulates basement fault reactivation. In the experiments involving silicone putty at the base of the sand pile, a thin (5–8 mm) layer of this was placed directly onto the clay blocks. Alternating layers of blue and white sand were then sieved onto the models. The models did not have side walls and the sand was allowed to drape over the edge of the models as shown in Fig. 1(b & c). Edge effects occur where the sand pile drapes over the edge of the model and the layering is not horizontal. These parts of the model were not used.

During extension, the basal putty layer extended as the rubber sheet stretched in a uniform manner. Extension of the putty was transmitted to the overlying clay blocks and sand layers. Alternating layers of red and white sand were then added to maintain a horizontal upper surface, thereby simulating syn-tectonic sedimentation, and the filling of fault-created depressions.

A camera mounted above the deformation apparatus photographed the top surface of the models at various stages throughout the experiment. To highlight deformation in the models, photographic lights were set at low angles to the model. Faults that broke through to the surface and that dipped toward the light source appeared relatively brighter than the surrounding flat surface, whereas faults that dipped away from the light source had shadows cast by their scarps. This has the advantage that faults dipping in opposite directions can be distinguished in plan-view photographs.

The models were extended at a rate of 7 cm per hour until the length of the clay block configuration was 14 cm (28%) longer than the initial length. This represents about 7–14 km extension in nature (see following section on scaling). At the end of each experiment, the model was saturated with a water–gelatine mixture which set the sand hard and allowed it to be cut with a knife to expose serial cross-sections through the models. Sections were cut parallel to the bulk extension direction.

Scaling

In geological applications, analogue models are constructed in the laboratory in an attempt to reproduce structures analogous to those observed in natural systems at a much smaller scale. As was stressed by Hubbert (1937), the key to meaningful analogue modelling of earth processes lies in the proper scaling of model parameters. Weijermars *et al.* (1993) elaborate ...

"Structures in a scale model behave like those of a prototype if they had similar length scales before deformation provided that the force field, thus rheology, and boundary conditions are properly scaled. Proper scaling of the quantities controlling the force field will then ensure similarity between the model and its prototype in terms of stress magnitudes and trajectory patterns: a requirement for dynamic similarity. Patterns of stress trajectories will match if the non-dimensional equations governing the deformation process are the same." However, experimental modelling uses simplified versions of natural systems and will always exclude some aspect of the real material behaviour. Therefore, it would be foolish to expect models to be exact representations of the complex natural systems they model, and as stated by Johnson (1970), "...the value of experimentation in the mechanics of the earth materials is not to produce scale models, but rather, to investigate certain concepts ... and to stimulate the imagination of the experimenter". After observing the growth and evolution of faults in experiments, a geologist may be able to recognise the same general behaviour in the field, and thereby generate ideas about the evolution of the region. Nevertheless, a concerted effort was made in this study to scale the materials and processes.

The structural response of sedimentary rocks was modelled using dry quartz sand, which is a Coulomb material with an angle of internal friction $\phi = 30$–$32°$ (Krantz, 1991). This is similar to the angle of internal friction determined experimentally for rocks under low pressures and temperatures (i.e. brittle sedimentary rocks in the upper continental crust) (Byerlee, 1978). Sand of 300 μm grain size and a density of about 1600 kg m^{-3} was used in the experiments. Dry quartz sand is a frictional plastic material that deforms by slip along fault planes or narrow shear zones (Mandl, 1988; Krantz, 1991) and represents a good analogue for brittle sedimentary rocks in the upper continental crust (Horsfield, 1977; Byerlee, 1978). Because dry quartz sand fails according to a simple Mohr Coulomb-type failure criterion (which is unaffected by strain rate), experiments involving sand only can be run at any reasonable speed without a significant variation in the structural style expected. However, experiments involving silicone putty (which is strain-rate dependent) require careful consideration of the rate of deformation.

Two types of silicone putty were used in the experiments. Dow Corning 3179 Silastic Dilatant Compound (a high-viscosity silicone putty), was used as the basal layer. It was not specifically employed to represent the lower ductile crust, but may act in a similar way in that it accommodates the necessary sinking and rotation of the clay (basement) blocks during extension. Because this type of silicone putty lies beneath the clay blocks and is only there to accommodate movement of the clay blocks, its viscosity is irrelevant. Silbione silicone (formerly known as Rhodorsil Gomme), a lower viscosity polymer manufactured by Rhône–Poulenc, was used to simulate a basal ductile layer in a sedimentary sequence, such as an evaporite or shale. It has a viscosity of 3×10^4 Pa s and a density of 1140 kg m^{-3} (Weijermars *et al.*, 1993) or 2×10^4 Pa s and 1150 kg m^{-3}, respectively as suggested by Richard (1991).

Here we scale a hypothetical natural prototype down to model size by a factor of 1–2×10^{-5}. Thus the 50-cm clay block scales to between 25 and 50 km in nature. A putty layer of thickness 5–8 mm represents a ductile layer of thickness of between 250 and 800 m, and a 6 cm-thick sand pile represents a sedimentary overburden of between 3 and 6 km. If we use Richard's values for Silbione silicone, and a length scaling value of 1–2×10^{-5}, we can use an experimental rate of extension of 7 cm per hour to model a natural extensional rate of 3 cm per year applied to rocks of viscosity between 1.5×10^{18} and 4×10^{18} Pa s (see fig. 2 of Richard, 1991). Alternatively, if we assume a length scaling factor of 2×10^{-5}, an experimental rate of 7 cm h^{-1} can be applied to model a natural extensional rate of 1 cm to 7 cm per year applied to rocks of viscosity 0.5×10^{18} Pa s to 3×10^{18} Pa s, respectively (see fig. 2 of Richard, 1991). These values are consistent with the viscosities of evaporites estimated by Odé (1968), and also fit within the new values suggested by Weijermars *et al.* (1993). The ratio of viscosity between model and hypothetical prototype varies between 2.5×10^{13} and 2×10^{14}. We were restricted to an experimental extension rate of 7 cm h^{-1} as this is the slowest speed at which the screw-jack was capable of running. If we simulate a natural rate of 3 cm y^{-1} and use our length scaling factor of 1–2×10^{-5}, an experiment run for 2 h (14 cm extension = 7–14 km in nature), represents a real time value of between 233,000 and 467,000 y (i.e. a time scaling factor of about 1×10^{-9}). 14 cm extension in a 50 cm-long model equates to 28% extension in the model.

Dry Walker Ceramics white pottery clay was used to simulate the rigid crystalline basement blocks in the upper brittle crust. The cuts in the clay represent discontinuities such as pre-existing faults. The particular brand was chosen for its low shrinkage factor, which allowed the clay blocks to fit together after being shaped, cut and dried, and also allowed for the repetition of experiments without significant variation in block shape.

RESULTS

Extension in the models reactivated the faults in the clay, while the basal putty accommodated the subsidence and rotation of the clay blocks. When sectioned, offsets of the contrasting coloured sand layers clearly defined the positions of the cover faults. Sections were cut subparallel to the extension direction. Faults oblique to the extension direction were therefore also oblique to the sections, and only an apparent dip could be attained on such faults. Faults are numbered in figures and referred to by number in the text to aid explanation of their

evolution. The repetition of any particular experiment showed that there were sufficient similarities between experiments in both map/plan and section views to indicate that results were reproducible, allowing the following generalisations to be made.

Experiments without a ductile layer

Grabens developed in the cover in a pattern that matched that of the underlying basement faults (Fig. 2). Synthetic faults formed, slightly before the antithetic faults, parallel to and adjacent to underlying basement faults (#s 1, 3, 5 and 7). Cover faults above the oblique NE-trending basement faults (#s 3, 4, 5 and 6) initially developed with a right-stepping *en échelon* pattern which, with continued extension, joined to form continuous faults with small steps in their traces (Fig. 2). Section A–B intersects one of the oblique NE-trending basement faults and highlights a curved synthetic cover fault (#5) and a constant-dip antithetic fault (#6) that extends only slightly into the syn-extensional layers (Fig. 3). The synthetic fault has developed curvature such that it shows reverse offset of layers at shallow depth, a point where the fault is vertical near the boundary between the syn-tectonic and pre-tectonic layers, and normal offset of layers low in the section. Section A–B intersects the NW-trending graben (fault #s 7 and 8) at a point where both fault traces are straight.

In section, the graben that developed above the basement fault orthogonal to the bulk extension direction is bounded by two planar (constant dip) faults (#s 1 and 2). The synthetic fault (#1) dips at about 60° (steeper than the 40° basement-fault) and shows significantly more offset than the antithetic fault (#2, which dips at about 70°). Because these two cover faults are the only faults of the graben, this difference in offset results in a slight rotation of the graben block.

Removal of sand from the model showed that the individual basement blocks had moved and rotated during extension (Fig. 4).

Experiments with a ductile layer

Surface views (Fig. 5) show that the pattern of cover deformation does not mimic that of the basement faults as closely as experiments without the ductile layer. Initially, two W-dipping faults (#s 3 and 4) developed in an area without any parallel basement fault directly below. They have strikes that are slightly oblique to the bulk extension direction and step *en échelon*, with the tips of their traces terminating along a trend that is parallel to

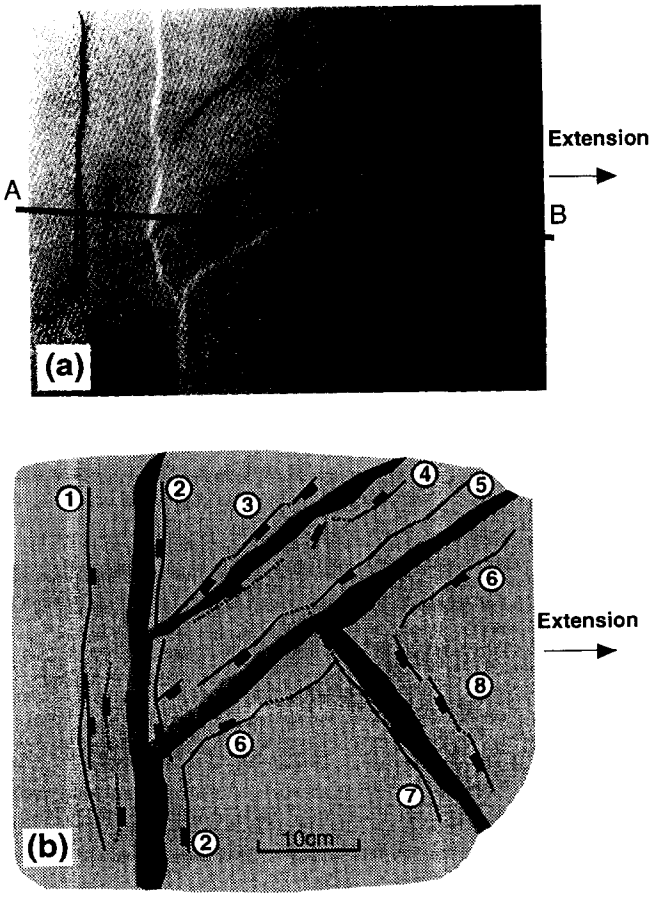

Fig. 2. Experiment without a ductile layer. (a) Plan-view photograph (illuminated from WNW) of deformed model top surface after 14 cm (28%) extension. Line A–B represents the position of the section in Fig. 3. (b) Line drawing of positions of fault scarps and their relation to basement faults after 14 cm (28%) extension. Faults with surface offsets < 0.5 mm are not mapped.

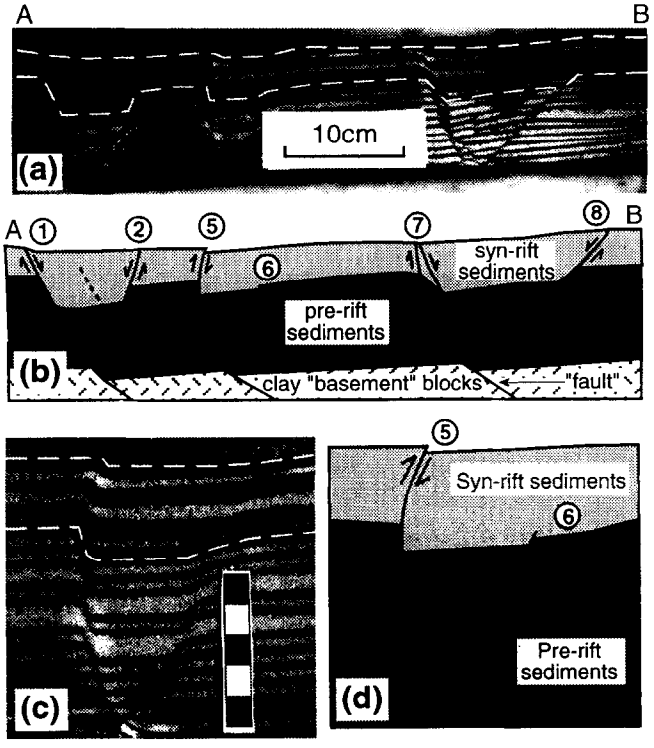

Fig. 3. (a) Photograph and (b) line drawing of cross-section A–B (Fig. 2a). (c) is a close-up photograph and (d) a line drawing, of the middle graben showing reverse offset across the curved synthetic fault (#5).

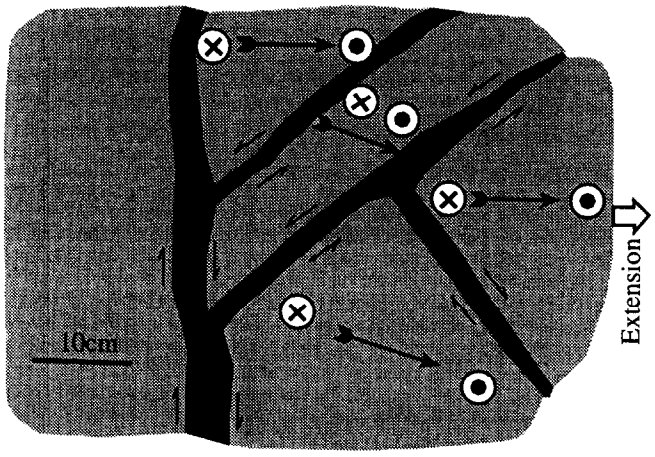

Fig. 4. Vector diagram of basement block movement after extension. Tailed arrows indicate relative block movement directions. Circles with crosses indicate downward movement and filled circles indicate upward movement. Half arrows indicate relative slip across faults.

and adjacent to the trend of an underlying oblique basement fault. The step of the two faults creates a small relay ramp between them, but with continued extension, fault #4 curved and intersected fault #3 (Fig. 5c & d).

Two E-dipping fault strands (#6) developed synthetic to, and stepped *en échelon* along, an underlying oblique basement fault. A few small-offset, close-spaced, parallel faults (#7) developed above the middle of the wedge-shaped basement block orthogonal to the bulk extension direction. One fault (#8) dipping in the opposite direction to fault #s 3 and 4 developed above a neighbouring basement block, again not parallel to any underlying basement fault, and connected with fault # 3 (Fig. 6b). Fault #3 has an opposite dip direction to #8 and the surface offset of each fault decreases as they approach each other (in map-view) until they meet at a point where there is no surface offset on either fault. A NNE-trending graben with irregular bounding fault traces resulted as fault #s 4 and 8 extended to the NNE.

Continued extension resulted in faults (#7) developing into one large fault, oriented orthogonal to the bulk extension direction. A graben developed above, and parallel to, the basement fault oriented orthogonal to the bulk extension direction. However, deformation was not as well developed in regions directly above basement faults oblique to the bulk extension direction.

Sectioning reveals that the graben above the basement fault orthogonal to the bulk extension direction is made up of a 60°-dipping synthetic (#1) and 60°-dipping antithetic (#2) fault. The synthetic fault soles at the top of the footwall basement fault, whereas the antithetic fault soles at the top of the hanging-wall basement fault.

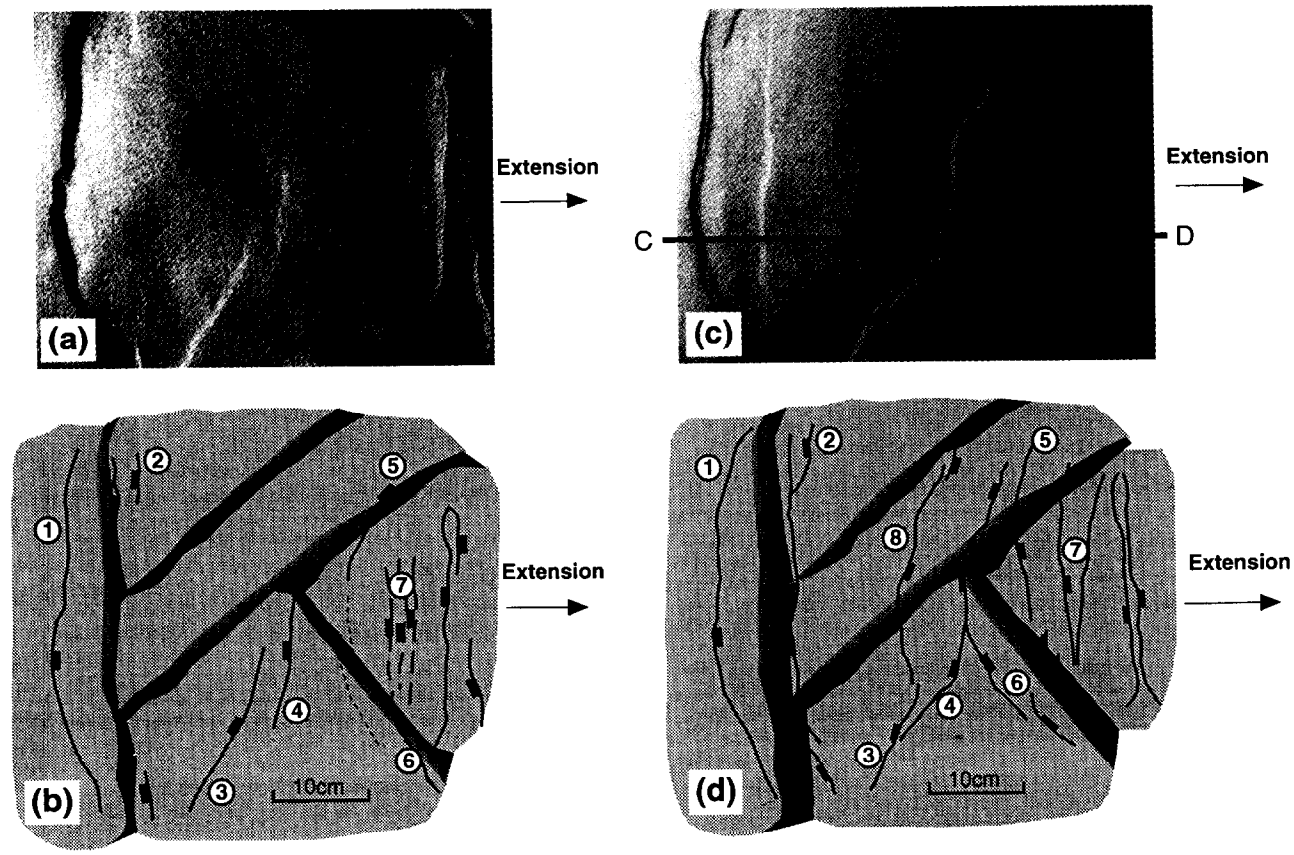

Fig. 5. Experiment with a ductile layer. (a) Plan-view photograph and (b) line drawing of fault positions and relation to basement faults of deformed model surface after 5 cm (10%) extension. (c) Plan-view photograph and (d) line drawing of fault positions and relation to basement faults of deformation of model surface after 14 cm (28%) extension. Faults with surface offsets < 0.5 mm are not mapped.

There is more offset on the synthetic fault than on the antithetic fault and, because these are the only two faults of the graben, the result is a rotation of the layers within the graben block (Fig. 6).

The NNE-trending graben consists of two planar faults of equal offset and angle of apparent dip (#s 4 and 8). The putty is deformed where these faults sole into it (Fig. 6), with the map-view pattern of deformation mimicking that of the cover faults.

In sections similar in position to A–B in Fig. 2(a), cover faults are not present above and parallel to basement faults oriented oblique to the extension direction. In other sections faulting is also minor above basement faults oblique to the bulk extension direction. Furthermore, faults that are present in these areas are of constant dip or have only minor curvature.

Removal of the sand from the clay basement again revealed that the individual clay basement blocks had moved and rotated (about a horizontal axis), as in the experiment without a basal ductile layer in the overburden (see Fig. 4).

DISCUSSION

Kinematics

The graben that developed above the orthogonal basement fault in experiments without a ductile layer in the overburden, can be likened to those modelled by Horsfield (1977). His experiments matched our imposed conditions in involving orthogonal movement on a 45°-dipping basement fault with no ductile layer in an overlying sand cover. In Horsfield's experiments, and in ours, the synthetic cover-fault rooted at the top of the basement fault and the antithetic fault rooted at the top of the basement hanging-wall where it met the basement fault (see Horsfield, 1977; Fig. 3a & c). However, a second synthetic fault in Horsfield's experiments developed, which we infer occurred because of the greater extension.

The synthetic fault above the orthogonal basement fault often displays more offset than the antithetic fault, which causes a rotation of the intervening graben block. This suggests that the synthetic fault accommodates both extensional strain and rotation, whereas the antithetic fault accommodates extensional strain only. This rotation may be associated with the rotation of the basement blocks (Fig. 4).

The curved (in section) fault that develops above an oblique basement fault in experiments without a ductile layer in the overburden (#5) may be likened to those modelled by Richard (1991), Richard and Krantz (1995) and Richard *et al.* (1995). The experiments they describe all involve oblique-slip movement which resulted in synthetic faults that are curved in section (Richard, 1991, fig. 6a; Richard and Krantz, 1995, fig. 12a; and Richard *et al.*, 1995 fig. 1). However, the experiments of these authors involved such faults within grabens above oblique basement faults, which we again infer resulted from the extension being greater than in our experiments. The curved faults modelled in our experiments also bear resemblance to curved precursor faults modelled, without oblique-slip movement, by Horsfield (1977, fig. 3a). However, no curved synthetic faults developed above the orthogonal basement fault in our models, suggesting that the curved faults were caused by oblique-slip movement.

We suggest that the initial right-stepping *en échelon* pattern of cover faults with a trend parallel and adjacent to oblique basement faults highlight a sinistral sense of shear on them and the underlying basement faults (Fig. 4). With continued extension, these cover faults linked to form continuous faults with irregular traces. It is possible that section A–B was cut across one of these steps or irregularities in the trace of an oblique cover fault (#5 Figs 2 & 3). Because not all synthetic faults above oblique basement faults show reverse movement, it is a possibility that such movement only developed in positions where such faults stepped. The reverse movement may have developed to accommodate or relay strain across the stepping fault.

The results of experiments involving a basal ductile layer in the overburden contrast with those of experiments without it. In the former, the pattern of deformation above the ductile layer is quite uniform and geometrically unlike that of the underlying basement faults. We suggest that the ductile layer partially decoupled the cover from the basement and infer that cover faulting was a response to widening of the model (i.e. thin skinned tectonics), with only minor influence from the underlying basement faults. Model widening caused roughly N–S striking extensional faults to form in the sand (sub-perpendicular to the E–W extension direction) (Fig. 5c & d), and sole and extend into the putty layer, localising strain in the process (Fig. 6).

As previously stated, however, the cover fault pattern does not indicate a total decoupling of cover from basement. Although more extension was needed to form the graben above the orthogonal basement fault when the ductile layer was present than when it was absent, eventually the graben developed. Figure 7 schematically illustrates how the graben block rotated, with more movement on the synthetic fault than the antithetic. Grabens that were not influenced by basement faults had equal offsets on straight (in section) bounding faults. We believe this is a response to the widening of the model without the need to accommodate any rotation. Moreover, we suggest that the small-offset *en échelon* stepping cover faults (#6, Fig. 5) which are parallel to the underlying basement faults, further highlight the influence of those basement faults (as described in experiments without a ductile layer in the cover).

Measurements of the movement directions of the clay markers after removing the sand layer illustrates the oblique-slip nature of movement of the basement blocks for both experiments (Fig. 4). We suggest that the direction of movement of each particular block is due to

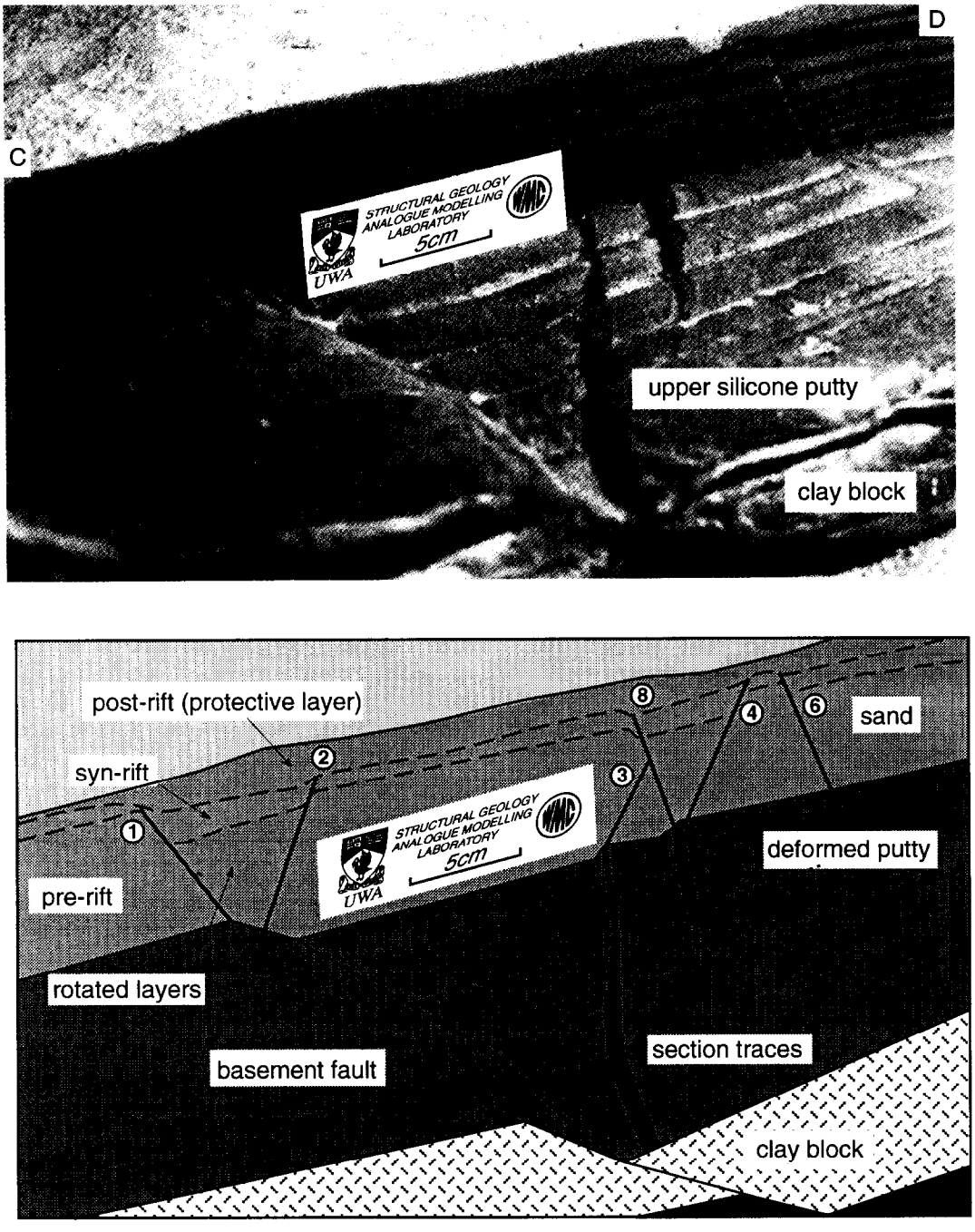

Fig. 6. (a) Oblique view of section across C–D (Fig. 5c) and (b) line drawing of same, showing relationship of cover faults and deformed putty after removal of the sand-layer only. The thin grooves are section traces and thick grooves show where cover faults have soled into the putty.

a combination of the bulk extension and dip-slip movement. Extension reactivates the faults and, as a block slides down a fault surface, it has a component of movement parallel to the bulk extension direction, and a component of dip-slip movement, i.e. an extension oblique to an existing basement fault generates an oblique-slip vector on that basement fault. Furthermore, because the basement block also rotates in the vertical plane as it slides, the putty thins across the resulting basement highs and thickens across basement lows (i.e. basement faults). The flow of silicone during faulting has also been modelled by, among others, Richard (1991) and Richard and Krantz (1995).

Cover faults above oblique basement faults were not as well developed in experiments without a basal ductile layer in the overburden as in experiments with the ductile layer present. Also, they were straight or had only minor curvature and did not show any reverse movement. We believe this is due to a combination of two factors. Firstly, N–S faults caused by widening of the model (thin

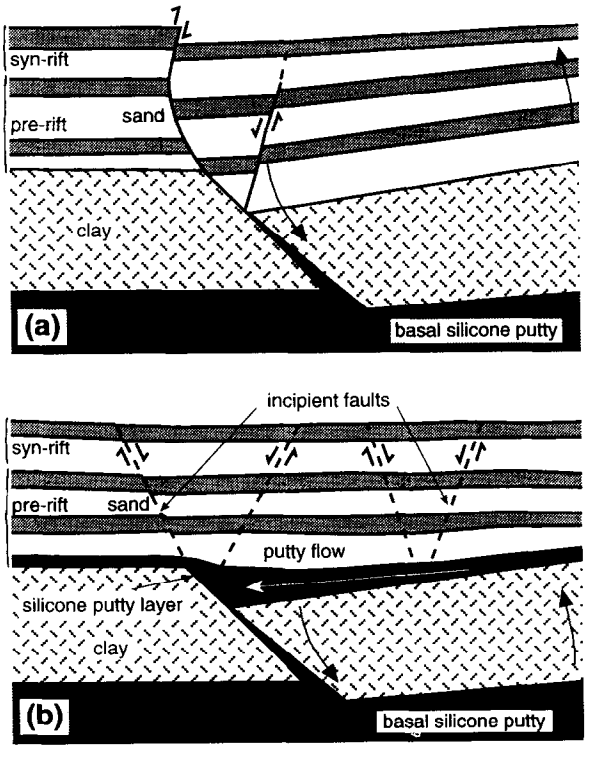

Fig. 7. (a) Experiment without a ductile layer. Schematic cross-section through a cover sequence above basement faults that are oblique to the bulk extension direction. (b) Experiment with a ductile layer. Schematic cross-section through the cover sequence above basement faults that are oblique to the bulk extension direction. See text for discussion.

skinned tectonics) probably accommodated most of the strain. Therefore, faulting to accommodate strain oblique to basement faults was not required. Secondly, the thickening of putty across the oblique basement faults would reduce the amount of displacement across the basement faults and overlying cover faults (Fig. 7b). This would also reduce the amount of oblique-slip movement in the cover and cover faults would not develop curved profiles.

Implications

Geologists should be cautious when studying regions which include ductile layers, such as shales or evaporites, within cover sequences deposited upon faulted basement. The deformation accommodated in the cover may seem to be geometrically independent and unrelated to the deformation accommodated in the basement. During regional extension, covers with ductile layers within them (especially thick basal layers) may decouple the cover sequence from the underlying faulted basement. This will result in faults with strikes perpendicular to the extension direction even if underlying oblique basement faults are reactivated (i.e. thin skinned tectonics). Covers without a ductile layer are more likely to develop faults that are influenced by underlying reactivated basement faults, and the strikes of such cover faults cannot be used to determine the orientation of regional stress. Sets of normal faults with differing strike may be easily confused with structures resulting from two or more phases of crustal extension with differing orientations of maximum extension direction. An origin due to basement fault reactivation in a single event may be distinguished from superposed events as one fault set does not always cross-cut the other (see Fig. 2). Additionally, faults in one orientation may either terminate against faults in another orientation, or merge with them.

The strikes of faults developed in covers with basal ductile layers cannot be used to determine accurately the orientation of regional stress unless the cover is fully decoupled. If the cover is still partially coupled, basement faults may still influence cover faulting (as in our experiments). The degree to which the basement faulting affects cover faulting will depend on the thickness and viscosity of the basal ductile layer. The thicker the basal ductile layer, the less influence basement faulting will have and vice versa. Thus, the thicker the ductile layer, the more accurately regional stress can be predicted from the strikes of cover faults that developed during deformation. Alternatively, ductile layers of relatively low viscosities would not need to be as thick as more viscous ductile layers to have the same decoupling effect. Furthermore, the style of cover faulting may vary with time. The decoupling layer may be thinned during extension allowing the basement to increase its influence on the cover.

This experimental program has only modelled a hypothetical case, varying one parameter. It is possible for natural situations to have totally different strain rates, thickness ratios and viscosities. Furthermore, the arrangement of brittle and ductile layers may differ. A ductile layer does not need to be located at the base of the sequence for it to affect the deformation style of the overlying strata. A sedimentary overburden may contain several ductile layers such as shales and evaporites throughout the sequence. The deformational response to the reactivation of underlying basement faults will differ in sediments above and below ductile layers. As previously stated, the degree to which such layers affect the deformation style will depend on layer thicknesses and viscosities. The deformation below the ductile layer would be restricted to areas directly above the reactivated basement faults as modelled in experiments without a ductile layer. However, given a thick enough ductile layer or one with low enough viscosity, it is unlikely that these faults would propagate into the sediments above it. Deformation would be dispersed through the ductile layer and deformation above it would be geometrically unrelated to the basement faults. This has important consequences when extrapolating faults to depths. One may not simply be able to project surface faults to depth, without knowing something about the composition of the cover sequence. Such a change in fault style and orientation over a given horizon may be incorrectly interpreted as evidence for an unconformity.

The results from these experiments also have implications for economic geologists. Fault systems provide the essential plumbing for focussing epithermal fluid flow from deeper reservoirs and magmas up to shallow stratigraphic levels (Henley, 1991). A better understanding of the relationship between faults in a cover sequence and those in the basement may therefore help to understand fluid-migration pathways. It is therefore important for exploration of commercial accumulations of both minerals (in the form of epithermal gold deposits as well as syn-sedimentary base-metal mineralisation) and hydrocarbons. For example, it is possible that the intersections of basement faults and cover faults will be areas that experience mixing of fluids from different sources. Dixon *et al.* (1989) mentioned that geochemical studies of ore deposits from the Carboniferous base-metal mineralising system in central Ireland showed that at least two distinct fluids were mixed. The two fluids correspond to shallow S-rich basinal fluids and a metal-rich deeply circulated basement fluid. They noted that other large Pb–Zn districts such as SE Missouri, Tri-State and the Upper Mississippi Valley have isotopic systematics that indicate a fluid mixing origin. These areas of basement- and cover-fault intersections are therefore prime base-metal exploration targets.

Frequently, seismic or drill hole data cannot provide adequate information about the orientation of basement faults. However, if a geologist suspects a certain basement fault geometry, say from aeromagnetic interpretation, and knows the mechanical stratigraphy of the cover sequence, analogies with experimental models can be made. The experimental structural models add weight to the geologist's argument, and predictions of the positions of basement fault and cover fault intersections can then be improved.

An understanding of the structural complexities within sedimentary basins, such as the reason for localisation of structures in particular areas (the nature of basement control) and the detailed tectonic evolution of particular structures, will ultimately help in the search for commercial hydrocarbon accumulations.

CONCLUSIONS

The experiments highlighted major differences in deformation style associated with changes in cover sequence composition. Results show that the rheology, hence composition, of a cover sequence has an impact on the orientation and localisation of cover faults above reactivated basement faults.

Experiments without a ductile layer in the cover sequence resulted in the development of grabens that were restricted to areas directly above basement faults. The strikes of such grabens cannot be used to determine the orientation of regional stress. In map-view, the pattern of cover faults 'fitted' the basement fault pattern perfectly. Synthetic and antithetic faults of grabens above oblique basement faults initially developed with en èchelon-stepping patterns, highlighting the oblique-slip nature of such faults. These linked to form continuous faults with irregular traces. In section, the synthetic faults of such grabens were curved and in some places showed reverse movement at shallow depths, further highlighting their oblique-slip nature. Block movement analysis shows that oblique-slip movement occurred on oblique basement faults and we infer that the curved (in section) faults developed as a result of this oblique-slip movement being transmitted into the cover. No curved faults developed above the orthogonal basement fault that had purely dip-slip movement, substantiating the inference that oblique slip movement caused the curved cover faults.

The results of experiments involving a basal ductile layer in the overburden differed remarkably from those of experiments without it, even though extension in both experiments was similar. The cover fault pattern was quite uniform with faults striking roughly N–S (subperpendicular to the E–W extension direction) and did not match the pattern of the underlying basement faults. Deformation was reduced above basement faults because faults that developed during widening of the model (N–S strikes) in random locations accommodated most of the strain, lessening the amount of strain to be accommodated above basement faults. Furthermore, the flow of putty across basement faults reduced the amount of offset across such basement faults and therefore also in the overlying cover faults. Faulting was influenced by both E–W extension and the reactivation of basement faults, and the final cover fault pattern was controlled by a combination of the two effects.

The influence that reactivated basement faults have on faulting in a cover containing a basal ductile layer is controlled by the thickness and viscosity of that layer. The thicker the layer, or the lower the viscosity of the layer, the more chance it has of decoupling the cover from basement. Only strikes of faults developed in covers that have been fully decoupled from the basement can be used to determine the orientation of the regional stress that caused them.

Cover and basement faults are likely to focus fluids during reactivation. Therefore, modelling the relationships between cover and basement faults during deformation in specific systems may help to understand fluid-migration pathways within those systems. This may ultimately lead to the discovery of commercial accumulations of hydrocarbons and minerals.

Acknowledgements—Experiments were funded by the Australian Research Council through a Collaborative Research Grant with Western Mining Corporation to L. Harris and M. Dentith. The authors thank Western Mining Corporation for permission to publish this paper. Silbione silicone putty was provided by J. Scott. Special thanks to Anthony Gartrell, David Byrne, Michael Dentith and Andrew Carmichael for their contributions, and also to B. Vendeville and P. Richard for their most helpful reviews of the manuscript.

REFERENCES

Byerlee, J. (1978) Friction of rocks. *Pure and Applied Geophysics* **116**, 615–626.

Davy, P., Sornette, A. and Sornette, D. (1990) Some consequences of a proposed fractal nature of continental faulting. *Nature* **348**, 56–58.

Dixon, P. R., Rye, D. M. and Le Huray, A. P. L. (1989) Fluid mixing and the origin of large Zn–Pb–Ba deposits (abstr.). In *Geological Society of America, 1989 annual meetings*, Dymock, R. F., chairperson et al. *Abstracts with Programs. Geological Society of America* **21**, 7

Henley, R. W. (1991) Epithermal gold deposits in volcanic terranes, In *Gold Metallogeny and Exploration* ed. R. P. Foster, pp. 133–164. Blackie, Glasgow and London.

Horsfield, W. T. (1977) An experimental approach to basement-controlled faulting. *Geologie en Mijnbouw*. **56**, 363–370.

Hubbert, M. K. (1937) Theory of scale models as applied to the study of geological structures. *Bulletin of Geological Society of America* **48**, 1459–1520.

Johnson, A. M. (1970) *Physical Processes in Geology*. Freeman, Cooper and Co., San Francisco.

Krantz, R. W. (1989) Fault inversion in scaled experimental models. *Bulletin of Geological Society of America* **21**, 176.

Krantz, R. W. (1991) Measurement of friction coefficients and cohesion for faulting and fault reactivation in laboratory models using sand and sand mixtures. *Tectonophysics* **188**, 203–207.

Mandl, G. (1988) *Mechanics of Tectonic Faulting: Models and Basic Concepts*. Elsevier, Amsterdam.

Odé, H. (1968) Review of mechanical properties of salt relating to salt-dome genesis. In *Diapirism and Diapirs* ed. J. Braunstein and G. D. O'Brien. American Association of Petroleum Geologists. pp. 53–78.

Richard, P. (1991) Experiments on faulting in a two-layer cover sequence overlying a reactivated basement fault with oblique-slip. *Journal of Structural Geology* **13**, 459–469.

Richard, P. and Krantz, R. W. (1995) Experiments on fault reactivation in strike-slip mode. *Tectonophysics* **188**, 117–131.

Richard, P. D., Naylor, M. A. and Koopman, A. (1995) Experimental models of strike-slip tectonics. *Petroleum Geoscience* **1**, 71–80.

Tchalenko, J. S. (1970) Similarities between shear zones of different magnitudes. *Bulletin of geological Society of America* **81**, 1625–1640.

Tron, V. and Brun, J.-P. (1991) Experiments on oblique rifting in brittle–ductile systems. *Tectonophysics* **188**, 71–84.

Vendeville, B., Cobbold, P. R., Davy. P., Choukroune, P. and Brun, J.-P. (1986) Physical models of extensional tectonics at various scales. In *Continental Extensional Tectonics*, ed. P. P. Coward, J. F. Dewey and P. L. Hancock. Special Publication of Geological Society London. **28**, 95–108.

Vendeville, B. C., Hongxing, G. and Jackson, P. A. (1995) Scale models of salt tectonics during basement-involved extension. *Petroleum Geoscience* **1–2**, 179–183.

Weijermars, R., Jackson, M. P. A. and Vendeville, B. (1993) Rheological and tectonic modeling of salt provinces. *Tectonophysics* **217**, 143–174.